www.czasopisma.pan.pl PAN www.journals.pan.pl

ARCHIVES of FOUNDRY ENGINEERING

ISSN (2299-2944)
Volume 21
Issue 2/2021

81 – 88

10.24425/afe.2021.136102

12/2

Published quarterly as the organ of the Foundry Commission of the Polish Academy of Sciences

Comparison of Microstructure and Mechanical Properties of Cast Steel Carried out on Cast-on Samples and Samples Cast Separately

B.E. Kalandyk *, R.E. Zapała
AGH University of Science and Technology, Department of Cast Alloys and Composites Engineering, Faculty of Foundry Engineering, ul. Reymonta 23, 30-059 Krakow, Poland
* Corresponding author. E-mail: bk@agh.edu.pl

Received 29.01.2021; accepted in revised form 10.06.2021

Abstract

The results of microstructure examinations and UTS, YS, El, RA carried out on low-carbon cast steel containing 0.15% C. The tests were carried out on specimens cut out from samples cast on a large-size casting and from samples cast in separate foundry moulds. It has been shown that significant differences in grain size observed in the material of the separately cast samples and cast-on samples occur only in the as-cast. In the as-cast state, in materials from different tests, both pearlite percent content in the structure and mean true interlamellar spacing remain unchanged. On the other hand, these parameters undergo significant changes in the materials after heat treatment. The mechanical properties (after normalization) of the cast-on sample of the tested cast steel were slightly inferior to the values obtained for the sample cast in a separate foundry mould. The microscopic examinations of the fracture micro-relief carried out by SEM showed the presence of numerous, small non-metallic inclusions, composed mainly of oxide-sulphides containing Mn, S, Al, Ca and O, occurring individually and in clusters.

Keywords: Mechanical properties, Metallography, Heat treatment, Cast steel

1. Introduction

Low-carbon cast steel is characterized by very good plastic properties (El, RA, KV) and is widely appreciated for satisfactory weldability and high magnetic properties. Unfortunately, because of the carbon content not exceeding 0.2%, it has relatively low strength properties (UTS, YS) [1-3]. These properties of the cast steel can be improved by metallurgical treatment, i.e. the use of complex deoxidizers and modification of non-metallic inclusions by introducing CaSi or rare earth metals (REM) into the bath [4-8]. Good effects are obtained when into the metal bath are introduced elements strongly refining and precipitation hardening the microstructure, generally known under one common name of microadditives e.g. Nb, Ti, V [9]. The type of the heat treatment of steel castings, matched to the casting dimensions and wall thickness, is also important, as it controls the grain size and austenite transformation products and, as a final result, the properties obtained [10, 11].

With its high mechanical properties and low production costs, combined with the readily available charge materials, low-carbon cast steel is widely used for castings that are expected to carry low or variable loads, which include castings for the industry

branches, such as railway, marine (rudders, anchors, or parts of ship hulls) or electrical (motor casings) [1, 3]. In recent years, due to low production costs, carbon steel castings have been increasingly replacing welded steel elements in marine structures, e.g. on drilling platforms and in the broadly understood offshore sector [12].

Because of variations in the size and wall thickness of steel castings, and hence in the casting solidification and cooling rate, the mechanical properties of cast steel are determined either on cast-on samples or on samples cast separately, where the sample dimensions and method of metal feeding are usually described in the technical documentation. This is particularly important in the production of massive castings.

This article presents the results of tests carried out on low-carbon cast steel using specimens cut out from samples cast on a large-size casting and from samples cast in separate foundry moulds.

2. Test material

Low-carbon cast steel melted under industrial conditions in an electric arc furnace was used in the tests. The chemical composition of the tested cast steel is given in Table 1. Argon agitation for approx. 480 s was used for the post-furnace melt treatment in a ladle (the mass of the melt was 26 Mg). Moulds were poured with molten metal at a temperature of approx. 1560°C. The casting was knocked out from the mould in accordance with the technological guidelines developed.

The samples (cuboid with size of 90 x 270 x 270 mm) were cast on a large-size casting and additionally they were cast in a separate foundry mould (the "clover" type sample). The samples cast on the large-size casting were placed in such a way as to ensure the cooling conditions similar to the cooling conditions of a massive casting (the sample size of 90 mm corresponded to the predominant wall thickness of the casting). The simulation carried out in the ProCast program showed that, in the range of crystallization temperatures, the cooling rate was similar in both tests. On the other hand, in the solid state, below the solidus temperature, the lower was the temperature, the greater was the difference in the cooling rate between the tests samples. The cast-on samples were stress-relieved to reduce to minimum the stresses arising during casting solidification and cooling. Both cast-on sample (cut off from the casting) and the "clover" sample were subjected to normalizing at 930°C.

Table 1.
Chemical composition of the tested low-carbon cast steel

Grade	Content of elements, wt.%									
	C	Si	Mn	P	S	Ni	Cr	Cu	Al	other
230-450W*	0.25	0.60	1.20	max. 0.035	max. 0.035	max. 0.40	max. 0.04	-	-	-
Melt	0.15	0.40	1.05	0.011	0.010	-	0.03	0.10	0.045	Ti+V+Nb < 0.02%

*/ according to PN-ISO 3755-1994 [2]

Specimens for metallographic examinations and mechanical tests were prepared from the heat treated material. Metallographic examinations using a light microscope Leica MEFUM and a JEOL 5500LV and HITACHI S-3400N scanning electron microscopes were carried out on the specimens prepared in a standard way, i.e. etched with 2% nital. The static tensile test was carried out with a ZWICK machine according to the procedure described in PN-EN ISO 6892 [13]. The tests were carried out on three specimens taken from each of the tested materials.

On the SEM images of the tested samples taken at a magnification of 500x using an image analysis software (ImageJ, 1.52av), the percentage of pearlite and the grain size were determined in the tested material. Moreover, using SEM images taken at a 5000x magnification, the mean distances between the plates in randomly selected pearlite colonies were measured.

On the SEM images of the examined samples, using image analysis software (ImageJ, 1.52av), the grain size in the tested material and the content of pearlite were determined. As, according to [14], the number of incisions along the secant length can be a measure of the grain size, the random secant method, adapted in accordance with the guidelines given in [14] for calculations in two-phase structures (e.g. ferritic-pearlitic), was used to determine this parameter. Measurements were taken in ten randomly selected areas at a magnification ensuring the visibility of several dozen measured objects on the image. The total area of measurement was approximately 0.3 mm^2. Moreover, using SEM images, the mean true interlamellar spacing was determined in randomly selected pearlite colonies. For measurements, the images with clearly visible pearlite lamellae taken at a magnification of 5000x were used. A circle with a specific diameter was superimposed on the randomly selected cross-section of a lamellar structure, while calculations were based on assumptions presented in the literature [15].

3. Experimental results

3.1. Microstructure

The as-cast microstructure of the tested low-carbon steel is composed of ferrite and pearlite (Figs. 1 and 2). At higher magnifications, the needle-like form of Widmannstätten ferrite is visible, characteristic of the thick sections of the casting and the slow process of solidification and cooling (Figs. 1 and 2).

Comparing microstructures obtained in the cast-on sample and in the sample cast separately, a higher degree of structure refinement was observed in the sample cast separately, resulting mainly from differences observed in the solid-state cooling of both samples in furan sand moulds (simulation results - ProCast).

Carrying out the heat treatment recommended for carbon cast steel, i.e. normalizing, resulted in the refinement of both ferrite and pearlite, but the expected homogenization of microstructure was not achieved (Figs. 3 and 4). This sometimes happens when the heat treatment is carried out under industrial conditions. Failure to meet the heat treatment parameters results in an incomplete homogenization of the microstructure, which has happened in this particular case.

The results of the research on grain refinement, pearlite content and mean true interlamellar spacing in the sample cast-on and in the sample cast separately are presented in Table 2.

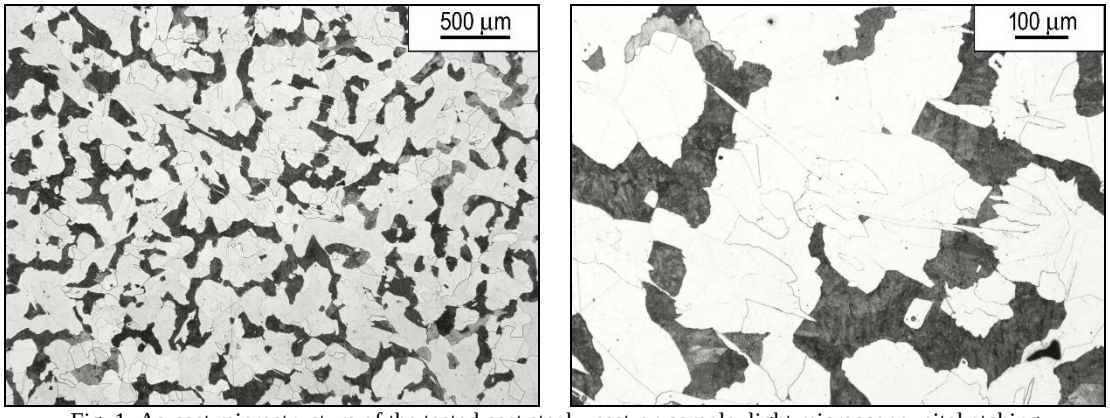

Fig. 1. As-cast microstructure of the tested cast steel - cast-on sample, light microscope, nital etching

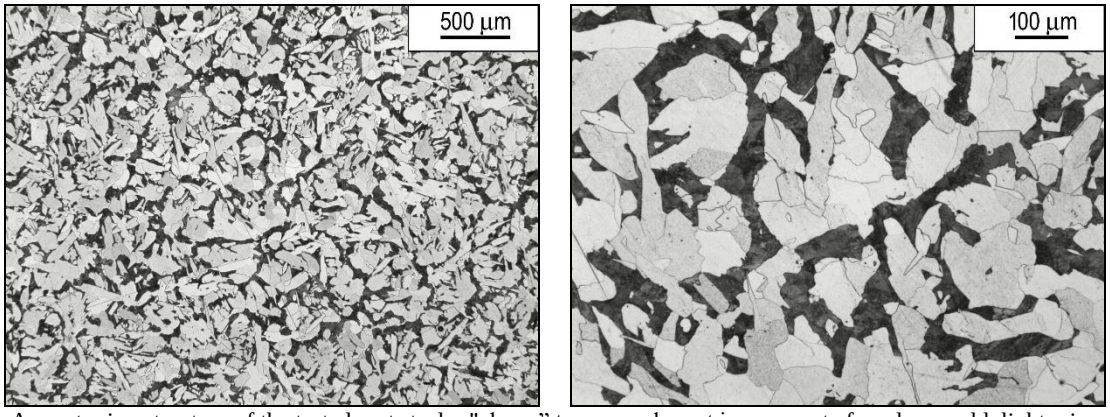

Fig. 2. As-cast microstructure of the tested cast steel – "clover" type sample cast in a separate foundry mould, light microscope, nital etching

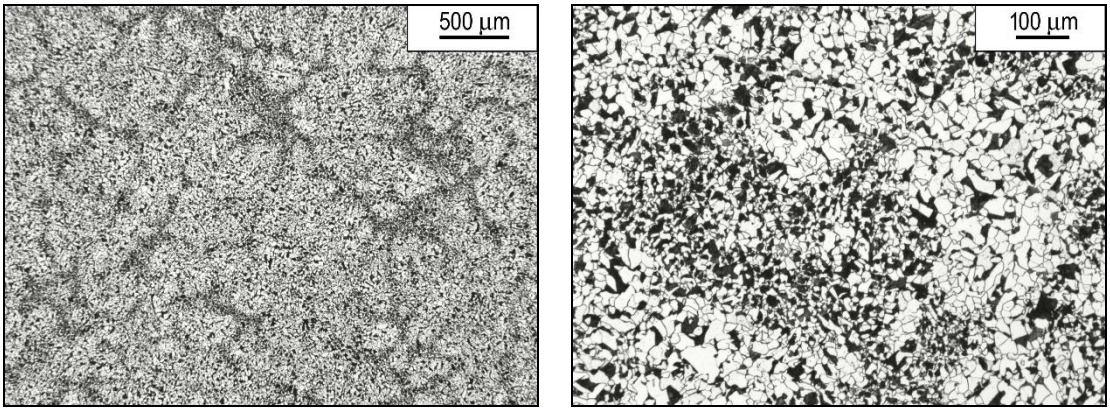

Fig. 3. Post - normalizing microstructure of the tested cast steel - cast-on sample, light microscope, nital etching

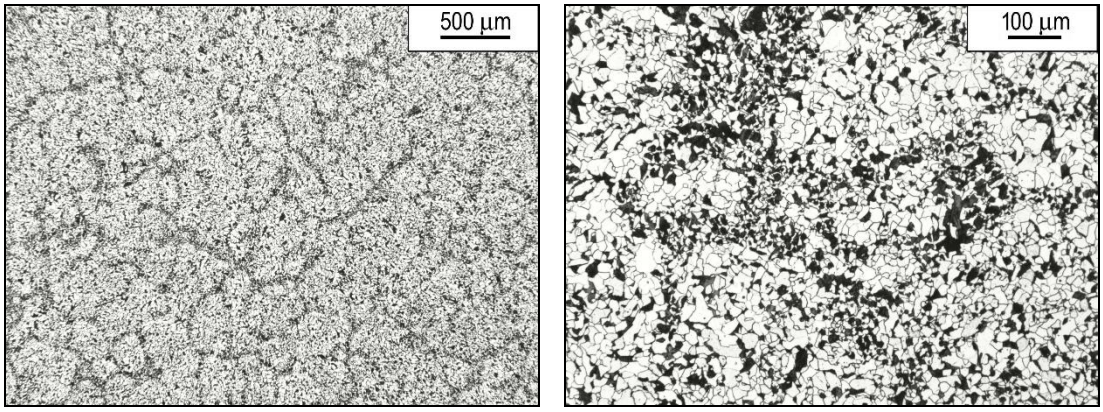

Fig. 4. Post - normalizing microstructure of the tested cast steel – sample cast separately, light microscope, nital etching

Table 2.
Grain size, pearlite content and mean true interlamellar spacing in the tested cast steel

	Grain size, µm		Pearlite content, %		Mean true interlamellar spacing, µm	
	As-cast state	Normalizing	As-cast state	Normalizing	As-cast state	Normalizing
Cast-on sample	50.5	10.2	28.4	24.6	0.21	0.16
Sample cast separately	32.0	9.8	30.2	22.0	0.20	0.15

Figure 5 shows pearlite present in the structure of the cast-on sample, while Figure 6 shows pearlite present in the sample cast separately.

Significant differences in grain size observed in the material of the separately cast sample and cast-on sample occur only in the as-cast / initial state. Moreover, it was found that the application of heat treatment affected the grain size refinement, pearlite content in the structure and mean true interlamellar spacing.

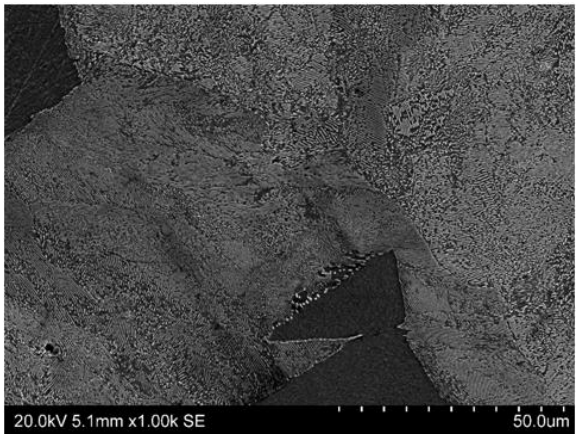

a)

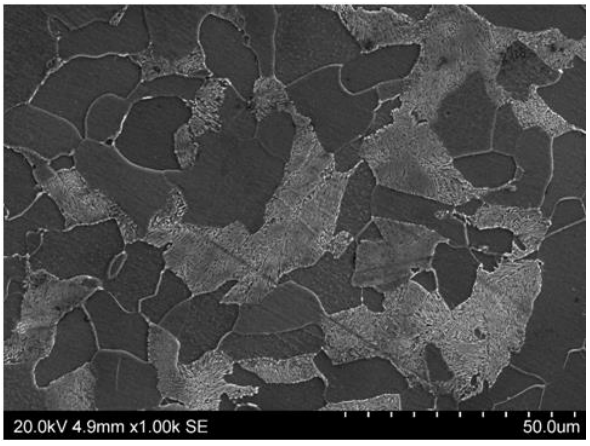

b)

Fig. 5. The image of pearlite in the tested cast steel – a) as-cast and b) after normalizing treatment - cast-on sample; SEM

The differences in the amount of pearlite after normalizing treatment compared to the initial state (cast-on sample and "clover") are due to the heterogeneous microstructure obtained after normalizing (Figs. 3 and 4), resulting from some minor deficiencies in the correct performance of heat treatment under industrial conditions. Despite the fact that before starting the measurement of the amount of pearlite, the required number of grid applications was determined [14], it was not possible to fully eliminate the effect of the above-mentioned heterogeneities on the obtained results.

a)

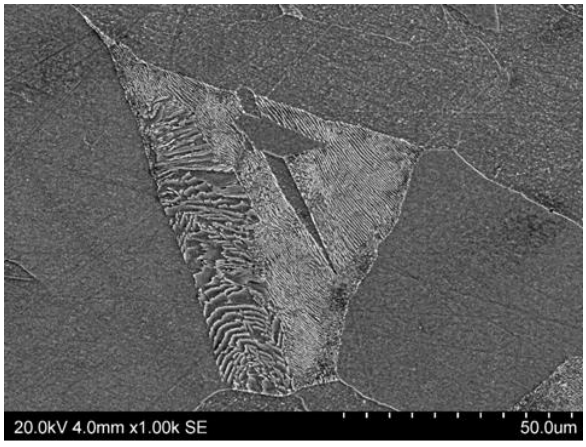

b)

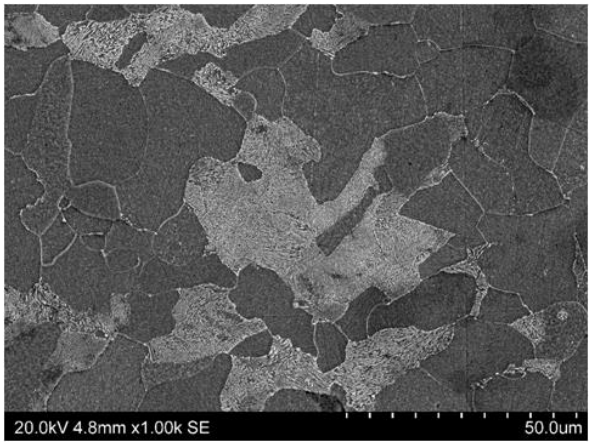

Fig. 6. The image of pearlite in the tested cast steel – a) as-cast and b) after normalizing treatment - sample cast separately; SEM

3.2. Static tensile test

Strength tests were carried out on heat-treated specimens cut out from the cast-on sample (samples 1÷3) and from the sample cast separately (samples 4÷6). The test results are given in Figures 7 and 8. It was shown that the values obtained for the specimens cut out from the cast-on sample were slightly inferior to the results obtained for the specimens cut out from the sample cast in a separate foundry mould (Fig. 8). In both cases, however, the UTS values were in the range of 472-496 MPa and exceeded the lower limit required by the standard for this type of cast steel (450-600 MPa according to [2]). YS values slightly exceeded 300 MPa (min. 230 MPa, [2]). In turn, the El values ranged from 33-37% (min. 22%), while the RA values ranged from 61-70% and doubled the minimum value specified in the standard (min. 31%) [2].

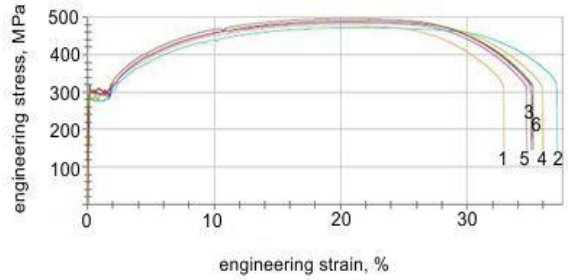

Fig. 7. Tensile curves plotted for the cast-on samples (samples 1÷3) and samples cast separately (samples 4÷6)

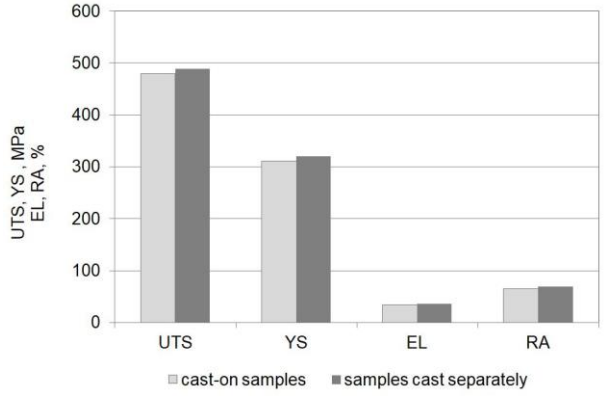

Fig. 8. Average values of UTS, YS, El and RA obtained for the tested cast steel after normalizing

Since for the tested cast steel grade the obtained values of UTS and YS approached the lower limit values, visual and microscopic analysis of randomly selected fractures was carried out. Under the conditions of static tensile test, all the specimens fractured in a fully ductile mode with "necking" in the place of fracture (Fig. 9a) forming a cup-and-cone shape [16]. The macro- and microscopic analysis of the fractures confirmed the strong plastic deformation of the tested cast steel observed in the specimens cut out from both cast-on samples and samples cast separately (Figs. 9 and 10). Additionally, the fractures were characterized by a matt surface with high roughness. SEM examinations confirmed the occurrence of ductile fracture in the central part of the specimen with characteristic pits (dimples) of different diameters, where cracks usually tend to spread in the direction perpendicular to the action of maximum tensile stresses, forming the cup-and-cone shaped failure surface (cracks formed by tearing mode). Then, as a result of local changes in the state of stress, the fracture mode changes into shear cracking (usually at an angle of 45° to the stretching direction) and is observed in the outer layers of the specimen (Figs. 9a and 10a).

The observations of the fracture surfaces showed that in many pits (dimples) there were non-metallic inclusions of various shapes, sizes and distributions, their size reaching even 10 μm. The same inclusions also occurred in clusters (Figs. 9c, d and 10c, d), which might be the cause of faster decohesion of the material and result in lower strength properties of the tested cast steel. According to the mechanism by which the voids surrounding the

inclusions are joined together and thus define the fracture path of the material, it can be concluded that non-metallic inclusions play an important role in fracture initiation. Thus, reducing the content of inclusions by appropriate secondary metallurgy may increase both strength and fracture toughness of the material [17-18]. Most of the non-metallic inclusions had a compact, globular-like shape. The analysis of the chemical composition has revealed that these were mainly complex precipitates, i.e. sulphide-oxides containing besides Mn and S also Al and Ca oxides (Table 3, 4). The presence of Ca in these complex inclusions may be due to the presence of CaSi in the metal bath, used as a modifier of non-metallic inclusions in the post-furnace treatment [3].

The SEM examinations of the fractures have shown that, as a result of uniaxial stretching, the pits (dimples) extend in the direction of the dominant axial stresses, forming equiaxial pits (Fig. 9d,10d) characteristic for the middle part of the fracture, i.e. "cup bottom." Such pitting geometry was not found in the fractures of the specimens subjected to impact tests.

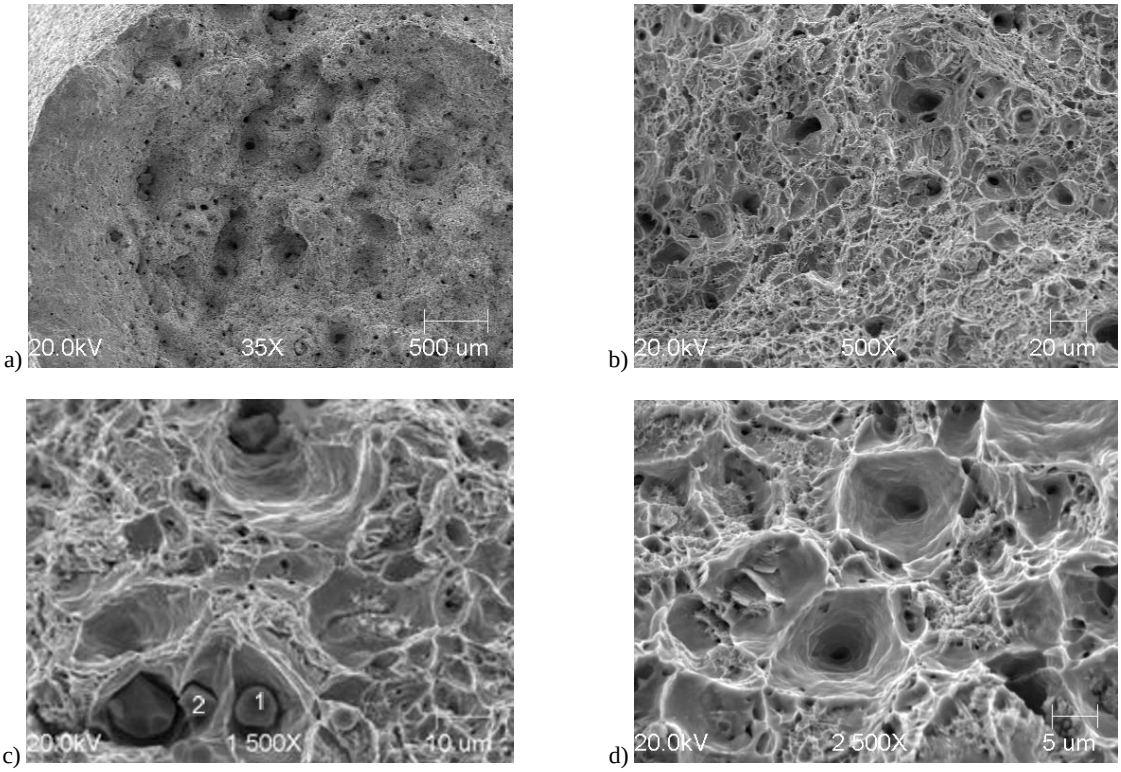

Fig. 9. Example of microstructure in the fracture of specimen subjected to static tensile test: a - cast-on sample; b, c, d - cup bottom; SEM

Table 3.
Analysis of the chemical composition of the precipitates present in the fracture

Points	Elements, wt. %					
	O	Al	Ca	Mn	S	Fe
1 – Fig. 9b	23.6	42.3	7.9	8.1	11.0	7.1
2 – Fig. 9b	8.8	26.9	10.3	23.4	20.8	9.8

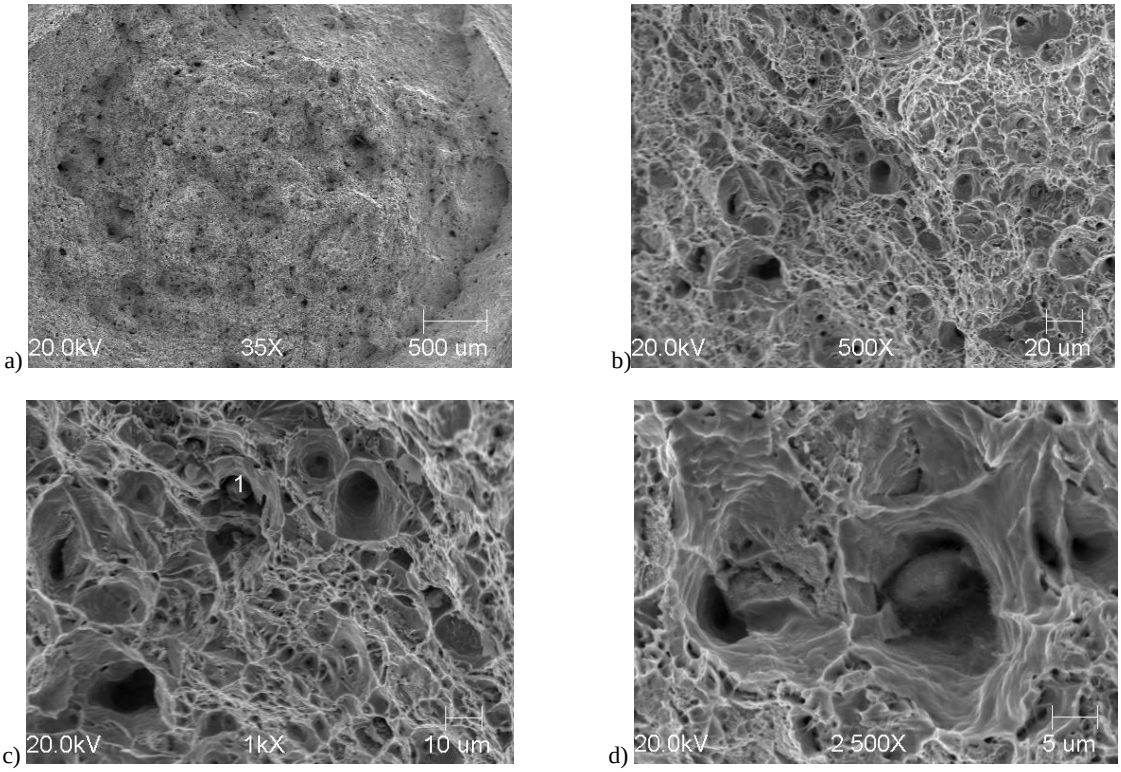

Fig. 10. Example of microstructure in the fracture of specimen subjected to static tensile test: a - sample cast separately; b, c, d – cup bottom; SEM

Table 4.
Analysis of the chemical composition of the precipitates present in the fracture

Point	Elements, wt. %					
	O	Al	Ca	Mn	S	Fe
1 - Fig. 10c	28.6	43.9	7.3	6.1	5.9	8.2

4. Conclusions

Based on the results of the studies, it was found that:

- Differences in grain size were observed in the tested cast steel in the initial state between sample cast on a large-size casting and sample cast separately. Similar differences were not observed in the content of pearlite and in the mean true interlamellar spacing.
- The strength properties of the cast-on sample of the tested cast steel were slightly inferior to the values obtained for the sample cast in a separate foundry mould.
- Under static tensile conditions, the tested cast steel cracked in a ductile mode typical for low-carbon steel and cast steel, with the reduction in area called "necking" in the rupture zone. Fractographic studies did not reveal any significant differences between the cast-on samples and samples cast separately.

Acknowledgements

This work has been partially executed under a Research Project P1.1.1-PG-09-001.

References

[1] Kniaginin, G. (1977). *Metallurgy and casting of steel*. Katowice: Śląsk. (in Polish).
[2] Standard PN-ISO 3755-1994. Cast carbon steels for general engineering purposes.
[3] Głownia, J. (2017). *Metallurgy and technology of steel castings*. Sharjah: Bentham Books. ISBN: 978-1-68108-571-5.
[4] Kasińska, J. (2017). Effects of rare earth metal addition on wear resistance of chromium-molybdenum cast steel. *Archives of Foundry Engineering*. 17(3), 63-68. ISSN: 1897-3310.

[5] Lis, T. (2009). *High purity steel metallurgy*. Gliwice: Wyd. Politechniki Śląskiej. (in Polish).
[6] Torkamani, H., Raygan, S., Mateo, C. G., Rassizadehghani, J. & Palizdar, Y. et al. (2018). Contributions of rare earth element (La, Ce) addition to the impact toughness of low carbon cast niobium microalloyed steels. *Metals and Materials International*. 24(4), 773-788. DOI:10.1007/s12540-018-.0084-9.
[7] Bartocha, D., Suchoń, J., Baron, Cz. & Szajnar, J. (2015). Influence of low alloy cast steel modification on primary structure refinement type and shape of nonmetallic inclusions. *Archives of Metallurgy and Materials*. 60(1). 77-83. DOI:10.1515/2015-0013.
[8] Żak, A., Zdonek, B., Adamczyk, M., Szypuła, I., Kutera, W. & Kostrzewa, K. (2015) Technology for manufacturing large – size steel castings for applications under extreme operating conditions. *Prace IMŻ*. 2: 21-28.
[9] Najafi, H., Rassizadehghani, J. & Halvaaee, A. (2007) Mechanical properties of as-cast microalloyed steels containing V, Nb and Ti. *Materials Science and Technology*. 23, 699-705. https ://doi.org/10.1179/17432 8407X17975 5.
[10] Miernik, K., Bogucki, R. & Pytel, S. (2010) Effect of quenching techniques on the mechanical properties of low carbon structural steel. *Archives Foundry Engineering*. 10 (SI 3), 91-96.
[11] Brooks, Ch. R. (1999). *Principles of the heat treatment of plain carbon and low alloy steels*. Materials Park: ASM International.
[12] Bolouri, A., Tae-Won, Kim & Chung, Gil Kang. (2013). Processing of low-carbon cast steels for offshore structural applications. *Materials and Manufacturing Processes*. 28: 1260-1267. DOI: 10.1080/10426914.2013.792424.
[13] Standard PN-EN ISO 3755-1994. 6892-1:2009. Metallic materials. Tensile testing. Part 1: Method of test at room temperature.
[14] Ryś, J. (1983). *Quantitative metallography*. AGH. (in Polish).
[15] Vander Voort, G. F. (1984). Measurement of the interlamellar spacing of pearlite. *Metallography*. 17: 1-17. https://doi.org/10.1016/0026-0800(84)90002-8.
[16] Wyrzykowski, J., W., Pleszakow, E., Sieniawski, J. (1999). *Metal deformation and fracture*. Warszawa: WNT. ISBN 83-204-2341-4. (in Polish).
[17] Maciejny, A. (1973). *The fragility of metals*. Katowice: Śląsk. (in Polish).
[18] Pacyna, J. (1986). Effects of nonmetallic inclusions on fracture toughness of tool steels. *Steel Research*. 57(11), 586-592. https://doi.org/10.1002/srin.198600830.